

# Performance Analysis of Feature Extraction Approach: Local Binary Pattern and Principal Component Analysis for Iris Recognition system

C D Divya<sup>1</sup> and Dr. A B Rajendra<sup>2</sup>

<sup>1</sup>AP, DoCS, VVCE, Mysuru, Karnataka, India

<sup>2</sup>Prof, DoIS, VVCE, Mysuru, Karnataka, India

\*Correspondence: C D Divya; Email: divyacd@vvce.ac.in

**ABSTRACT-** Many techniques have been proposed for the recognition of Iris. Most of them are single resolution techniques which results in poor performance. In this paper, feature extraction approaches like local binary pattern and principal component analysis assimilation has been offered. For classification, Support Vector Machine has been used. This paper compares the efficiency of two popular feature extraction methods Principal Component Analysis and Local Binary Pattern using two different iris databases CASIA and UBIRIS. The models were tested using 200 iris images. Statistical parameters like F1 score and Accuracy are tested for different threshold values. Our proposed method results with accuracy of 94 and 92%, is obtained for using Local Binary Pattern for CASIA and UBIRIS data set respectively. The Receiver Operating Characteristic Curve has been drawn and Area under Curve is also calculated. The experiment has been extended by varying the dataset sizes. The result shows that LBP achieves better performance with both CASIA and UBIRIS databases compared to PCA.

**General Terms:** Iris Recognition, True Positive, True Negative.

**Keywords:** Area Under Curve, Local Binary Pattern, Iris, Principal Component Analysis, Feature Extraction, F1 Score, Receiver Operating Characteristic Curve, Support Vector Machine.

## ARTICLE INFORMATION

**Author(s):** C D Divya and Dr. A B Rajendra

**Received:** 26/03/2022; **Accepted:** 27/04/2022; **Published:** 05/05/2022;

**e-ISSN:** 2347-470X;

**Paper Id:** IJEER220326;

**Citation:** 10.37391/IJEER.100201

**Webpage-link:**

<https://ijeer.forexjournal.co.in/archive/volume-10/ijeer-100201.html>



**Publisher's Note:** FOREX Publication stays neutral with regard to Jurisdictional claims in Published maps and institutional affiliations.

## 1. INTRODUCTION

The authentication of a person is of high importance in modern days [1]. Other than passwords and magnetic cards, authentication using biometric system is based on bodily or behavioral characteristics of a person. The physical characteristics such as palm print, fingerprint, face and iris recognition are proved to be accurate and fast. These characteristics are unique to an individual and remain stable through life, and the pattern variability is high among different persons make iris very fascinating for use as biometric system. A biometric system enables the identification of a person using distinct feature or characteristic exhibited individual person. The Biometric systems are designed for recognition by taking various physical traits as input such as palm prints, fingerprints, face, and the iris [2]. The iris is the coloured circle located around the pupil which includes number of randomly distributed structures which are not mutable and hence iris is quite different from other approach [3]. Earlier, iris biometrics recognition system was roughly advised from 2001 [4]. The original algorithm for iris identification works with analysis of texture [5]. The algorithm uses codes which

are generated using two-dimensional Gabor wavelet. The accuracy achieved is more compared to other methods. The important work done by Wildes [6] has adopted algorithm which uses applications of the Gaussian filters for the purpose of recognition and here, eyelids were modelled using parabolic arcs. Boashash and Boles [7] have proposed a method which has adopted zero-crossings. In wavelet transform, zero crossings are computed at different resolutions of circles of the iris which concentric. Signals with single dimensional are used to correlate with some important features using various dissimilarity functions. Same kind of approach has been presented which has adopted discrete dyadic wavelet transform and showed better efficiency [8]. The Multi-resolution Independent Component Identification (M-ICA) has acceptable ability to generate the iris features. According to authors accuracy of the system is comparatively low since the M-ICA does not work efficiently with class-separability. Chen and Yuan have proposed a new approach for generating the features of iris using fractal dimension [9]. The iris part has been divided into small parts and the features in the form of iris templates are generated. These generated templates known as iris code are then applied to the neural networks for the matching purpose. Robert et. al. have proposed a method for achieving localization and feature extraction using Integral-differential operators along with a Hough Transform[10]. Here, code for iris has been generated using both emergent frequency and instantaneous phase.

Li Ma. et. al. [11] have adopted HAAR-Wavelet transform for features extraction in iris. The transformation has been used on the image to generate a feature vector. To classify the vectors, two approaches namely weight vector initialization and winner

selection methods are adopted [12]. The recognition capability of classification methods are dependent on feature quality and the size data used for training. The features are generated from shape and texture of segmented parts. Karu et al. [13] presented an approach to achieve automatic identification of textured parts and the categorization uses statistical measures. The Co-occurrence approach is claimed to be the best for classification of texture by Connors and Harlow [14]. The iris structure can be classified with the help of coherent Fourier spectra using optical transmission [15]. The iris biometric designed by Hamed Ranjzad [16] has adopted Principal Component Analysis (PCA) for feature extraction. Here, authors attempted different illumination and noise level during the iris image acquisition process.

Furthermore, local-based approaches require less number of samples for analysis [24]. If Local Binary Pattern (LBP) descriptors are used straight away, review illustrates that, prove to be analysis will become more effective for face image. Since this method was utilized for face representation [23], there has been a growing interest in LBP-based features for other representations also [25].

Here, we offer a method for extracting the best features of iris images for iris template classification using PCA and LBP. Main purpose to use LBP in conjunction with PCA is to minimize the iris template resolution.

## 2. MATERIALS AND METHODS

Fig. 1 shows the overall architecture of the work carried out. For feature extraction, two methods have been used and compared. One is PCA [17, 18] and another one is LBP. Here, CASIA and UBIRIS datasets have been used in the experiment. For classification, Support Vector Machine (SVM) approach has been utilized.

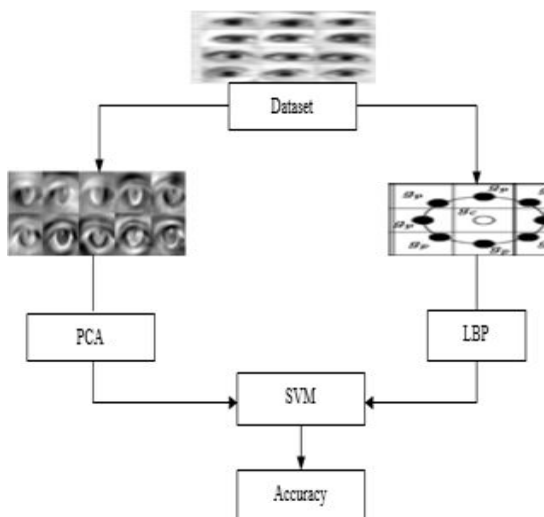


**Figure 1:** Over all architecture

### 2.1 Principal Component Analysis (PCA)

PCA is one of the most important aspects of linear algebra and it is widely being adopted for analysis purpose. Since it is simple and non-metric method it can be used in neuroscience as well

as in computer graphics. PCA guides how to reduce a high dimension data to a lower dimensional data to explore only the sufficient and important features. Extraction of the important features corresponding to the available data is the one of the major aspect of PCA [26]. During this, dimensionality of a data consisting of many correlated variables will get minimized. This is achieved by converting the data to a set of variables called the principal components (PCs). These PCs are independent and are arranged so that the first few components represent the most important features present in all the original variables.

### 2.2 Local Binary Pattern (LBP)

The number of methods has been developed to extract the useful features from iris images to perform iris biometric recognition. LBP [19, 20] is one among them. LBP make it is possible to represent the image texture and shape.

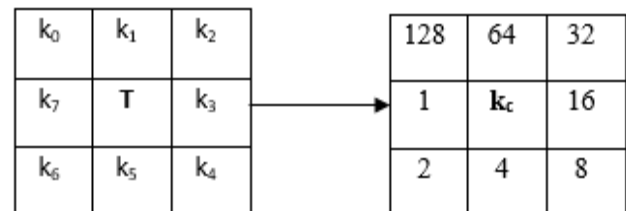


**Figure 2:** Local Binary Pattern

The concept of LBP was basically proposed by Ojala et al. [21]. The LBP operator uses pixel's neighbors and takes the Centre pixel value as a threshold as shown in Fig. 2. If a neighbor pixel has a larger gray value than the Centre pixel, then a '1' is set to the corresponding pixel otherwise '0' will be assigned. Final LBP code is evaluated by combining neighboring binary digits.

The value of the LBP code of a pixel ( $g_m, g_c$ ) is given by Eq. (1) and Eq. (2)

$$LBP_{M,N} = \sum_{m=0}^{M-1} l(g_m - g_c) 2^m \quad (1)$$

$g_m$  is the neighbor pixel value,  $g_c$  is the Centre pixel value or Threshold (T) value and  $m$  is the digit code with initial value 0 and final value 7.

$$l(x) = \begin{cases} 1, & x \geq T; \\ 0, & \text{otherwise} \end{cases} \quad (2)$$

$l(x)$  is the LBP feature matrix.

### 2.3 Support Vector Machine (SVM)

A SVM [22] which is used to classify data which are linearly separable is called linear SVM which is depicted in Fig. 3. Linear SVM searches for a hyper-plane with the maximum margin. Therefore, a linear SVM and hence called as a maximal margin classifier (MMC) [27]. Steps involved in finding the Maximum Margin Hyper-plane are discussed below:

1. Consider a problem of binary classification consisting of  $n$  training data.

2. Each tuple is represented by  $(X_i, Y_i)$  where  $X_i = (x_{i1}, x_{i2}, \dots, x_{im})$  corresponds to the attribute set for the  $i^{\text{th}}$  tuple (data in  $m$ -dimensional space) and  $Y_i \in \{+, -\}$  denotes its class label.

3. Given  $\{(X_i, Y_i)\}$ , a hyper-plane is generated which separates all  $X_i$  into two sides of it.

4. Consider a two-dimensional training data with attributes  $A_1$  and  $A_2$  as  $X = (x_1, x_2)$ , where  $x_1$  and  $x_2$  are values of attributes  $A_1$  and  $A_2$ , respectively for  $X$ .

5. Equation of a plane in 2-D space can be written as  $0 + w_1x_1 + w_2x_2 = 0$  [e.g.,  $a_x + b_y + c = 0$ ] where  $w_0, w_1$ , and  $w_2$  are some constants defining the slope and intercept of the line. Any point lying above such a hyper-plane satisfies  $w_0 + w_1x_1 + w_2x_2 > 0$  similarly, any point lying below the hyper-plane satisfies  $w_0 + w_1x_1 + w_2x_2 < 0$

6. An SVM hyper-plane is an  $n$ -dimensional generalization of a straight line in two dimensions.

7. Euclidean equation of a hyper-plane in  $R_m$  is  $w_1x_1 + w_2x_2 + \dots + w_mx_m = b$  (3) where  $w_i$ 's are the real numbers and  $b$  is a real constant.

8. In matrix form, a hyper-plane thus can be expressed as  $W \cdot X + b = 0$  (4) where  $W = [w_1, w_2, \dots, w_m]$  and  $X = [x_1, x_2, \dots, x_m]$  and  $b$  is a real constant.

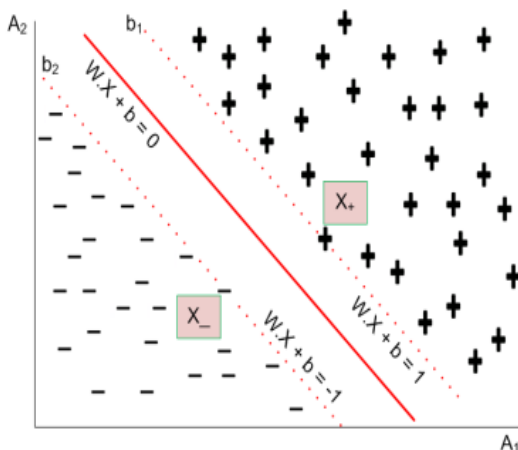


**Figure 3:** Computation of MMH

### 3. RESULTS AND DISCUSSION

For the computation processes we have used Intel core  $i5-i7$  generation CPU, with 8 GB system memory for implementing. Further we have considered CASIA and UBIRIS as two different iris data set. The size of CASIA will be  $320 \times 280$  and for UBIRIS it is  $200 \times 150$ . At the time of feature extraction this image of both the sets are resized to  $37 \times 50$ . Intruder and 100 genuine iris images have been used to conduct the experiment. The True Positive Rate (TPR), False Positive Rate and

Accuracy have been presented in *Table 1*. The accuracy has been evaluated over different probability threshold values.

**Table 1: Accuracy for different probability threshold**

Probability threshold	FP	FN	TP	TN	RECALL	PRECISION	TPR	FPR	ACCURACY
<b>PCA + SVM + CASIA</b>									
$\geq 0.0$	100	0	100	0	1	0.50	1	1	50%
$\geq 0.1$	88	2	98	12	0.98	0.53	0.98	0.88	55%
$\geq 0.2$	85	2	98	15	0.98	0.54	0.98	0.85	57%
$\geq 0.3$	75	3	97	25	0.97	0.56	0.97	0.75	61%
$\geq 0.4$	65	5	95	35	0.95	0.59	0.95	0.65	65%
$\geq 0.5$	18	5	95	82	0.95	0.84	0.95	0.18	89%
$\geq 0.6$	10	15	85	90	0.85	0.89	0.85	0.10	88%
$\geq 0.7$	8	30	70	92	0.70	0.90	0.70	0.08	81%
$\geq 0.8$	5	42	58	95	0.58	0.92	0.58	0.05	77%
$\geq 0.9$	1	70	30	99	0.30	0.97	0.30	0.01	65%
<b>PCA + SVM + UBIRIS</b>									
$\geq 0.0$	100	0	100	0	1	0.50	1	1	50
$\geq 0.1$	82	4	96	18	0.96	0.54	0.96	0.82	57
$\geq 0.2$	80	8	92	20	0.92	0.53	0.92	0.80	56
$\geq 0.3$	70	9	91	30	0.91	0.57	0.91	0.70	61
$\geq 0.4$	63	10	90	37	0.90	0.59	0.90	0.63	64
$\geq 0.5$	60	10	90	40	0.90	0.60	0.90	0.60	65
$\geq 0.6$	58	16	84	42	0.84	0.59	0.84	0.58	63
$\geq 0.7$	54	20	80	46	0.80	0.60	0.80	0.54	63
$\geq 0.8$	46	40	60	54	0.60	0.57	0.60	0.46	57
$\geq 0.9$	32	62	38	68	0.38	0.54	0.38	0.32	53

<b>LBP + SVM + CASIA</b>									
$\geq 0.0$	100	0	100	0	1	0.50	1	1	50
$\geq 0.1$	88	0	100	12	1	0.53	1	0.88	56
$\geq 0.2$	72	1	99	28	0.99	0.58	0.99	0.72	64
$\geq 0.3$	41	1	99	59	0.99	0.71	0.99	0.41	79
$\geq 0.4$	18	2	98	82	0.98	0.84	0.98	0.18	90
$\geq 0.5$	9	3	97	91	0.97	0.92	0.97	0.09	94
$\geq 0.6$	8	3	97	92	0.97	0.92	0.97	0.08	95
$\geq 0.7$	8	28	72	92	0.72	0.90	0.72	0.08	82
$\geq 0.8$	5	48	52	95	0.52	0.91	0.52	0.05	74
$\geq 0.9$	2	88	22	98	0.20	0.92	0.20	0.02	57
<b>LBP + SVM + UBIRIS</b>									
$\geq 0.0$	100	0	100	0	1	0.50	1	1	50
$\geq 0.1$	84	0	100	16	1	0.54	1	0.84	58
$\geq 0.2$	78	2	98	22	0.98	0.56	0.98	0.78	60
$\geq 0.3$	54	3	97	46	0.97	0.64	0.97	0.54	72
$\geq 0.4$	24	3	97	76	0.97	0.80	0.97	0.24	87
$\geq 0.5$	13	4	96	87	0.96	0.88	0.96	0.13	92
$\geq 0.6$	11	16	84	89	0.84	0.88	0.84	0.11	87
$\geq 0.7$	11	25	75	89	0.75	0.87	0.75	0.11	82
$\geq 0.8$	10	55	45	90	0.45	0.82	0.45	0.10	68
$\geq 0.9$	5	70	30	95	0.30	0.86	0.30	0.05	63

The ROC-Curve has been drawn for different combinations of methods and databases. Fig. 4 shows the ROC curves.

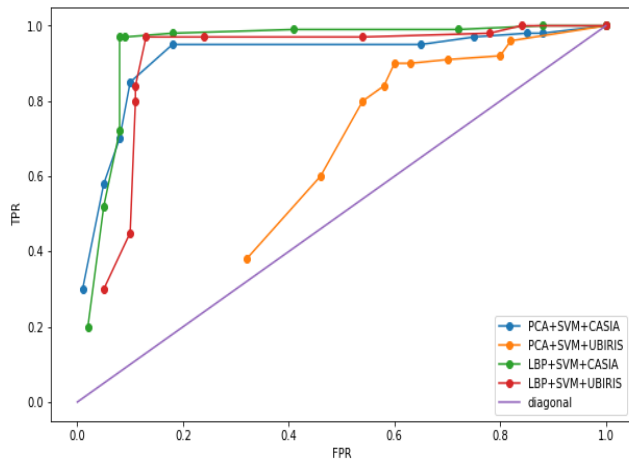


**Figure 4: ROC-Curve**

The Area under Curve (AUC) has been calculated for different combinations of feature extraction methods and classification methods along with two databases listed. The result obtained is presented in Table 2.

**Table 2: Area Under Curve (AUC)**

Method	AUC
PCA + SVM + CASIA	0.9125
PCA + SVM + UBIRIS	0.5518
LBP + SVM + CASIA	0.9395
LBP + SVM + UBIRIS	0.8962

The experiment has been conducted using different dataset size like 200, 400, 600 and 800. Even in this test case 50% of the images will be as intruder and remaining 50% of the images are considered as genuine to conduct the experiment. The result obtained for the above case conditions are presented in Table 3 and plotted as in Fig. 5. For different data set size, the accuracy remains high for the combinations PCA + SVM + CASIA, LBP + SVM + CASIA and LBP + SVM + UBIRIS.

**Table 3: Accuracy and AUC for different dataset size**

Method	Dataset size							
	200		400		600		800	
	Accuracy	AUC	Accuracy	AUC	Accuracy	AUC	Accuracy	AUC
PCA + SVM + CASIA	89%	0.9125	88%	0.9025	90%	0.9185	87%	0.8892
PCA + SVM + UBIRIS	65%	0.5518	64%	0.5416	68%	0.5698	58%	0.5123
LBP + SVM + CASIA	95%	0.9395	93%	0.9256	96%	0.9356	93%	0.9256
LBP + SVM + UBIRIS	92%	0.8962	90%	0.8756	91%	0.8562	91%	0.8562

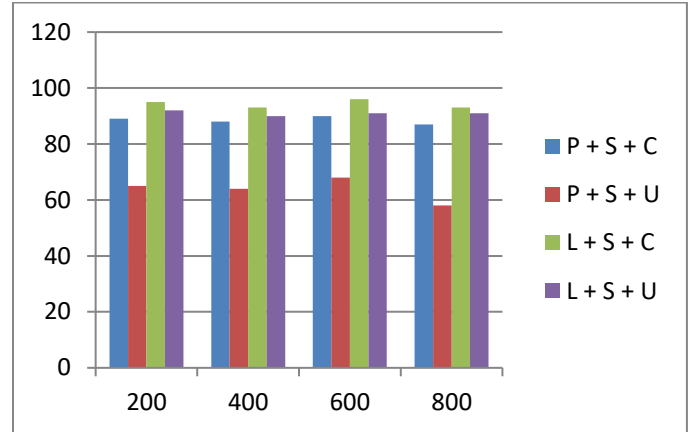


**Figure 5: Accuracy graph**

## 4. CONCLUSION

Experiment has been conducted to test the performance of PCA and LBP with two popular iris databases CASIA and UBIRIS. Support Vector Machine, which is a well-known feature-based classification approach has been adopted to carry out our research for both the methods. The models were tested using 200 iris images. In case of LBP, the AUC values obtained are 0.8962 and 0.9395 for CASIA and UBIRIS datasets respectively. In case of PCA, the AUC values are 0.9125 and 0.5518 for CASIA and UBIRIS datasets. The result shows that LBP achieves better performance with CASIA and UBIRIS compared to PCA. The experiment was extended for different dataset sizes of 400, 600 and 800. The result shows that LBP outperforms PCA with both CASIA and UBIRIS datasets. The work further may be extended for another approach of iris recognition like wavelet transform and suitable Hybrid approach.

## 5. REFERENCES

- [1] Jain A. K. Ross A. Prabhakar S. An introduction to biometric recognition. IEEE Transactions on Circuits and Systems for Video Technology, 14, January 2004 4 20, 1051-8215.
- [2] Sharma, Abhilash. (2015). Biometric System- A Review. International Journal of Computer Science and Information Technologies. 6. 4616-4619.
- [3] Sevugan, Prabu & Swarnalatha, P. & Gopu, Magesh & Sundararajan, Ravee. (2017). Iris recognition system. International Research Journal of Engineering and Technology.
- [4] Kak, & Neha, & Rishi, Gupta & Sanchit, Mahajan. (2010). Iris Recognition System. International Journal of Advanced Computer Sciences and Applications. 1. 10.14569/IJACSA.2010.010106.
- [5] Richard Yew Fatt Ng, Yong Haur Tay and Kai Ming Mok, "Iris recognition algorithms based on texture analysis," 2008 International Symposium on Information Technology, 2008, pp. 1-5, doi: 10.1109/ITSIM.2008.4631667.
- [6] R. P. Wildes, Iris recognition: an emerging biometric technology, Proceeding, pp s of the IEEE, vol.85, no.9, pp.1348-1363, p Se 1997.
- [7] Boles, Wageeh & Boashash, Boualem. (1998). A Human Identification Technique Using Images of the Iris and Wavelet Transform. Signal Processing, IEEE Transactions on. 46. 1185 - 1188. 10.1109/78.668573.
- [8] yankui sun, yong chen and hao feng, two-dimensional stationary dyadic wavelet transform, decimated dyadic discrete wavelet transform and the face recognition application, 9(3), 397-416, 2011.



- [9] XiaoZhou Chen, ChangYin Wu, LiangLin Xiong, Fan Yang, The Optimal Matching Algorithm for Multi-Scale Iris Recognition, Energy Procedia, Volume 16, Part B, 2012.
- [10] Hassanein, Allam S. et al. "A Survey on Hough Transform, Theory, Techniques and Applications." ArXiv abs/1502.02160 (2015).
- [11] Ma, Li & Tan, Tieniu & Zhang, Dai. (2004). Efficient Iris Recognition by Characterizing Key Local Variations. IEEE transactions on image processing: a publication of the IEEE Signal Processing Society. 13. 739-50. 10.1109/TIP.2004.827237.
- [12] Sousa, Celso. (2016). An overview on weight initialization methods for feedforward neural networks. 10.1109/IJCNN.2016.7727180.
- [13] J. Daugman, "How Iris Recognition Works," IEEE Trans. Circuits and Systems for Video Technology, vol. 14, no. 1, pp. 21-30, Jan. 2004.
- [14] Connors RW, Harlow CA. A theoretical comparison of texture algorithms. IEEE Trans Pattern Anal Mach Intell. 1980 Mar; 2(3):204-22. doi: 10.1109/tpami.1980.4767008. PMID: 21868894.
- [15] Hoxha, Julian & Stoja, Endri & Domnori, Elton & Cincotti, Gabriella. (2017). Multicarrier Digital Fractional Fourier Transform For Coherent Optical Communications. 10.1109/EUROCON.2017.8011073.
- [16] Ranjzad, Hamed & Ebrahimi, Afshin & Ebrahimnezhad, Hossein. (2008). Improving feature vectors for iris recognition through design and implementation of new filter bank and locally compound using of PCA and ICA. 10.1109/ISABEL.2008.4712612.
- [17] Mishra, Sidharth & Sarkar, Uttam & Taraphder, Subhash & Datta, Sanjoy & Swain, Devi & Saikhom, Reshma & Panda, Sasmita & Laishram, Menalsh. (2017). Principal Component Analysis. International Journal of Livestock Research. 1. 10.5455/ijlr.20170415115235.
- [18] Karamizadeh, Sasan & Abdullah, Shahidan & Manaf, Azizah & Zamani, Mazdak & Hooman, Alireza. (2013). An Overview of Principal Component Analysis. Journal of Signal and Information Processing. 10.4236/jsip.2013.43B031.
- [19] Song, Ke-Chen & YAN, Yun-Hui & CHEN, Wen-Hui & Zhang, Xu. (2013). Research and Perspective on Local Binary Pattern. Acta Automatica Sinica. 39. 730-744. 10.1016/S1874-1029(13)60051-8.
- [20] Huang, di & Shan, Caifeng & Ardabilian, Mohsen & Chen, Liming. (2011). Local Binary Patterns and Its Application to Facial Image Analysis: A Survey. IEEE Transactions on Systems, Man, and Cybernetics, Part C. 41. 765-781. 10.1109/TSMCC.2011.2118750.
- [21] Ojal T., Pietikinen M. and Harwood D., "A Comparative study of texture measures with classification based on featured distributions", Pattern Recognition, Vol 29, No. 1, pp.51~59, 1996.
- [22] Srivastava, Durgesh & Bhambhu, Lekha. (2010). Data classification using support vector machine. Journal of Theoretical and Applied Information Technology. 12. 1-7.
- [23] T. Ahonen, A. Hadid, and M. Pietikäinen, "Face recognition with local binary patterns," in Proc. Euro. Conf. Computer Vision (ECCV), 2004, pp. 469-481.
- [24] X. Tan, S. Chen, Z. Zhou, and F. Zhang, "Face recognition from a single image per person: a survey", Pattern Recognition, vol. 39, no. 9, pp. 1725-1745, 2006.
- [25] Kumar, G., Chowdhury, D. P., Bakshi, S., & Sa, P. K. (2020). Person Authentication Based on Biometric Traits Using Machine Learning Techniques. In IoT Security Paradigms and Applications (pp. 165-192). CRC Press.
- [26] Omran, Maryim, and Ebtesam N. AlShemmary. "An iris recognition system using deep convolutional neural network." In Journal of Physics: Conference Series, vol. 1530, no. 1, p. 012159. IOP Publishing, 2020.
- [27] Soliman, R.F., Amin, M., El-Samie, A. and Fathi, E., 2020. Cancelable Iris recognition system based on comb filter. Multimedia Tools and Applications, 79(3), pp.2521-2541.
- [28] Mayur Rahul, Namita Tiwari, Rati Shukla, Devvrat Tyagi and Vikash Yadav (2022), A New Hybrid Approach for Efficient Emotion Recognition using Deep Learning. IJEER 10(1), 18-22. DOI: 10.37391/IJEER.100103.



© 2022 by C D Divya and Dr. A B Rajendra. Submitted for possible open access publication under the terms and conditions of the Creative Commons Attribution (CC BY) license (<http://creativecommons.org/licenses/by/4.0/>).